Journal of University of Science and Technology Beijing
Volume 11, Number 3, June 2004, Page 263

Materials

Effect of VFe addition on hydrogen storage behavior of $TiMn_{1.5}$-based alloys

Xuebin Yu, Zhu Wu, Baojia Xia, Taizhong Huang, Jinzhou Chen, and Naixin Xu

Lab of Energy Science and Technology, Shanghai Institute of Microsystem and Information Technology, Chinese Academy of Sciences, Shanghai 200050, China

(Received 2003-04-26)

Abstract: The hydrogen absorption and desorption behavior of $TiMn_{1.25}Cr_{0.25}$ alloys with VFe substitution for partial Mn was investigated at 273, 293 and 313 K. It is found that VFe substitution increases their hydrogen storage capacity, decreases the plateau pressure and the hysteresis factor of their pressure-composition-temperature (PCT) curves. After annealing treatment at 1223 K for 6 h, $TiMn_{0.95}Cr_{0.25}(VFe)_{0.3}$ alloy exhibits a lower hydrogen desorption plateau pressure (0.27 MPa at 313 K) and a smaller hysteresis factor (0.13 at 313 K); the maximum and effective hydrogen storage capacities (mass fraction) are 2.03% and 1.12% respectively, which can satisfy the demand of hydrogen storage tanks for proton exchange membrane fuel cells (PEMFC).

Key words: TiMn-based alloy; hydrogen storage capacity; hysteresis; sloping factor; PEMFC

1 Introduction

Ti-Mn Laves phase alloys are one of the promising hydrogen storage materials with easy activation, good hydriding-dehydriding kinetics, high hydrogen storage capacity and relatively low cost. However, they have two critical drawbacks limiting their successful practical applications. One is their higher hydrogen absorption and desorption plateau pressure at room temperature, which is usually over 2 MPa. The other is a larger hysteresis between hydrogen absorption and desorption and a poor flatness of the hydrogen pressure plateau. In order to resolve these problems, much work has been done on improvement of hydrogen absorption and desorption characteristics of Ti-Mn_2-based multi-component alloys [1-3]. Recently, Park *et al.* [4] reported $(Ti_{0.75}Zr_{0.25})Mn_{0.8}Cr_{1.05}V_{0.05}Cu_{0.1}$ as a new alloy, which exhibits smaller hysteresis and less sloping pressure plateau. However, the plateau pressure of this alloy is still over 1 MPa, which is too high for proton exchange membrane fuel cells (PEMFC), the suitable plateau pressure for PEMFC is in the range of 0.1 MPa to 1 MPa [5].

Comparing with $TiMn_2$, $TiMn_{1.5}$ alloy has higher hydrogen storage capacity and better hydriding-dehydriding kinetics. Gamo *et al.* [6] examined the hydrogen plateau pressure of $TiMn_{1.5}$ alloys whose Mn is partially substituted by Cu, Co, Fe, Ni or V. They found that the plateau pressure decreases when Ni or V replaces Mn and the plateau pressure increases when Cu, Co or Fe replaces Mn. Hong *et al.* [7] reported that $TiMn_{1.25}Cr_{0.25}$ alloy has a higher hydrogen storage capacity, smaller hysteresis and flatter plateau, but the influence of simultaneous substitution of Cr, V and Fe for Mn in $TiMn_{1.5}$-based multi-compound alloys has not been systematically investigated.

In this work, the effect of VFe alloy addition on hydrogen storage characteristics of $TiMn_{1.25}Cr_{0.25}$ alloy was studied at 273, 293 and 313 K. V is known to form two types of hydride, monohydride, $VH_{\approx 1}$ and dihydride, $VH_{\approx 2}$. There is a very low equilibrium pressure of hydrogenation between V and $VH_{\approx 1}$ at room temperature. On the other hand, V has a high affinity for hydrogen. Therefore, it was expected that addition of V into $TiMn_{1.25}Cr_{0.25}$ would decrease its plateau pressure and increase its hydrogen storage capacity. VFe alloys instead of pure element V were chosen as melting raw materials in order to develop a hydrogen storage alloy with reasonable cost.

2 Experimental procedure

The composition of vandium-iron is as follows (mass fraction, %): V, 82.6; Mn, 0.07; C, 0.11; Si, 064; S, 0.016; P, 0.044; Fe, 16.52. The other original materials are pure metals. Alloy samples were prepared by magnetic levitation melting. 50 g of ingot was turned over and remelted for four times to insure its homogeneity. Besides the as-cast samples, other samples were undergone annealing treatment at 1223 k for 6 h as control. The nominal compositions of the alloys were designed as x=0, 0.1, 0.2, 0.3, 0.4 in the general for-

Corresponding author: Xuebin Yu, **E-mail:** yuxuebin@hotmail.com

mula $TiMn_{1.25-x}Cr_{0.25}(VFe)_x$. The exact compositions were analyzed by the induction coupled plasma (ICP) method. The ingots were crushed into powders with average particle size about 4 mm for PCT measurements and 30 μm for X-ray powder diffraction analysis. For the former, 3 g of powder samples were sealed into a stainless steel container, which was then evacuated at 473 k for 1h. The container was pressurized by 3 MPa of hydrogen gas, followed by absorption-desorption cycling about three or four times for activation. The hydriding and dehydriding behavior of the alloys was evaluated by PCT curves at various temperatures. The phase structure of all alloys under study was identified by a Philips PW1010 X-ray diffractometer with Cu K_α radiation.

3 Results and discussion

3.1 Phase structure

Typical elemental components for AB_2 alloys are A=Ti or Zr, and B=V, Cr, Mn, Fe, Co, Cu or Zn. The phase composition of the AB_2 alloys is correlated with the average number of outer electrons (ANOE). When ANOE is less than 5.4 no Laves phase could be formed for Ti and the C15 Laves phase is formed for Zr. If ANOE is between 5.4 and 7.0, the C14 Laves phase forms regardless of A=Ti or Zr. When ANOE exceeds 7.0 the C15 Laves phase forms.

Figure 1 shows XRD patterns of as-cast $TiMn_{1.25-x}Cr_{0.25}(VFe)_x$ (x=0, 0.1, 0.2, 0.3, 0.4) alloys. It is easily indexed on the basis of the hexagonal C14-Laves phase structure ($P6_3$ /mmc space group). There are no reflections corresponding to the cubic C15-Laves phase structure. The lattice constants a and c calculated from these patterns are summarized in **table 1**. Both lattice constants a and c of the hexagonal cell increase with increasing x and thus the unit cell volume increases too. It could be attributed to the fact that the atomic radius of V (0.192 nm) is larger than that of Mn (0.179 nm). Although the ANOE decreases as x increases, it is still in the range of 5.44-5.70. The XRD measurement results are in agreement with those reported in the literature [8].

Figure 2 is XRD patterns of as-cast and annealed $TiMn_{0.95}Cr_{0.25}(VFe)_{0.3}$ alloys, which shows that the crystal structure of the alloys doesn't change after annealing. However, the peaks of the annealed alloy becomes slightly sharper, which means that the homogeneity of the phase is improved by annealing treatment. In addition, the diffraction peaks of the annealed alloy shift toward a lower diffraction angle, which means that the lattice constants of the annealed sample are bigger than those of as-cast sample (see table 1).

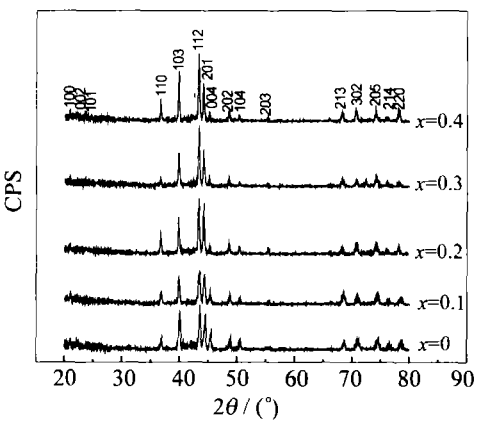

Figure 1 XRD patterns of as-cast $TiMn_{1.25-x}Cr_{0.25}(VFe)_x$ alloys.

Table 1 Lattice parameters and ANOEs of $TiMn_{1.25-x}Cr_{0.25}(VFe)_x$ alloys

Samples	a /nm	c /nm	V /nm^3	ANOE
x=0 (as-cast)	0.4851	0.7990	0.1628	5.70
x=0.1 (as-cast)	0.4852	0.8003	0.1632	5.64
x=0.2 (as-cast)	0.4876	0.8004	0.1648	5.59
x=0.3 (as-cast)	0.4889	0.8015	0.1659	5.54
x=0.3(annealing)	0.4895	0.8017	0.1663	5.54
x=0.4 (as-cast)	0.4896	0.8017	0.1664	5.44

3.2 PCT characteristics

The ideal hydrogen storage materials should have a larger hydrogen storage capacity, a smaller hysteresis and a flatter plateau. In order to explain absorption-desorpion characteristics of the alloys clearly, a schematic PCT curve is shown in **figure 3**. The curve involves a flat and wide pressure plateau with a slight slope. There is a discrepancy between absorption and desorption pressure which is defined as hysteresis. The effective hydrogen storage capacity, hysteresis and plateau effect are represented by an effective hydrogen desorption capacity (C_e), hysteresis factor (H_f) and sloping factor (S_f), which are defined as

$$C_e = w_{P_a=1\text{MPa}} - w_{P_d=0.1\text{MPa}} \quad (1)$$

$$H_f = \lg(P_a/P_d)_{H/M=0.5} \quad (2)$$

where w is the mass fraction of hydrogen in alloy, P_a is the hydrogen absorption pressure, P_d is the hydrogen desorption pressure, H/M is the atomic ratio of hydrogen to alloy.

$$S_f = \lg\left(P_{H/M=0.75} / P_{H/M=0.25}\right) \quad (3)$$

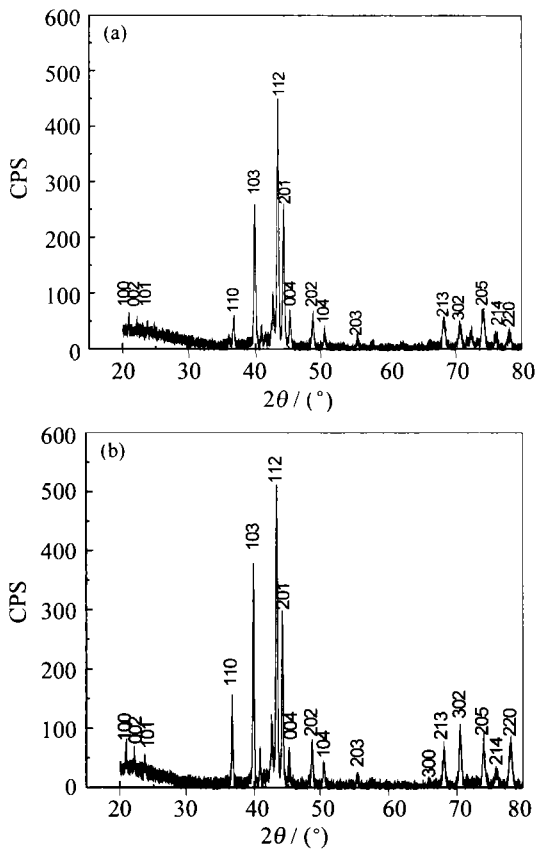

Figure 2 XRD patterns of $TiMn_{0.95}Cr_{0.25}(VFe)_{0.3}$ alloys: (a) as-cast; (b) annealed at 1223 K for 6 h.

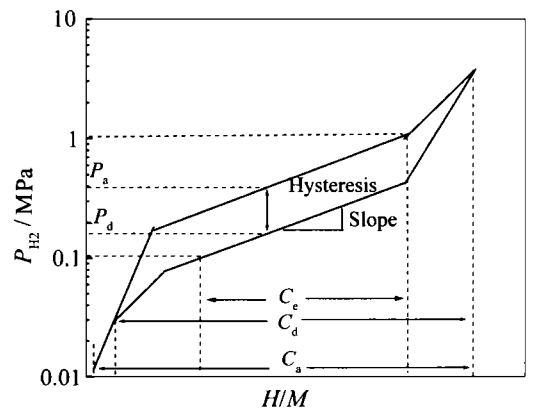

Figure 3 Schematic diagram of PCT for a hydrogen storage alloy.

Figure 4 show the PCT curves of as-cast $TiMn_{1.25-x}Cr_{0.25}(VFe)_x$ (x=0, 0.1, 0.2, 0.3, 0.4) at 273 K. The absorption-desorption characteristics are presented in **table 2**. The hydrogen capacity gradually increases with x from x= 0 to 0.3 but drops at x=0.4. The highest hydrogen absorption capacity (C_a), desorption capacity (C_d) and C_e are 2.0%, 1.69% and 0.89% at x=0.3 respectively. The plateau pressure and the hysteresis behavior are improved when x increases. However, the sloping factor S_a (absorption plateau) and S_d (desorption plateau) become poor.

The variation of plateau pressure can be interpreted by difference of the lattice parameters. With increasing x, the volume of the hexagonal cell (table 1) and the interstitial hole size increase [9], which logically leads to a decrease of both the plateau pressure and hysteresis. Such observations had already been done by Lee *et al* [10]. VFe substitution is effective on the increase of hydrogen capacity, which could be attributed to the stronger affinity of V with H compared with that of Mn. However, VFe substitution also results in a considerable increase of the slope of the plateau. This could be explained by using the local environment model proposed by Ivey and Northwood. In hexagonal AB_2 Laves phase, hydrogen atoms mainly occupy two kinds of interstitial site: $[A_2B_2]$ and $[AB_3]$. After V substitution, there are two types of B atoms: Mn and V. In the alloy there exist various interstitial sites, such as $[A_2MnV]$, $[A_2Mn_2]$, $[A_2V_2]$, which have different local environments and hence different hydrogen affinities. Interstitial sites such as $[A_2V_2]$ or $[AV_3]$ have a stronger affinity to hydrogen than $[A_2Mn_2]$ or $[AMn_3]$.

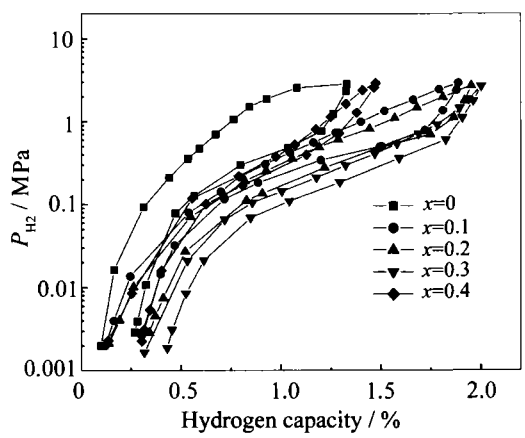

Figure 4 PCT curves of as-cast $TiMn_{1.25-x}Cr_{0.25}(VFe)_x$ alloys at 273 K.

A large amount of VFe substitution reduces the effective hydrogen capacity. This is because that the occupation of V on some B sites leads to the production of interstitial sites with a stronger affinity for hydrogen, which will form stable hydrides. On the other hand, the content of Fe also affects hydrogen storage capacity. this problem will be discussed elsewhere.

Annealing can improve the characteristics of hydriding-dehydriding reaction [11]. In lab, it is found that the alloys annealed at 1223 K for 6 h possess the best performance. **Figure 5** show PCT curves of as-cast and annealed $TiMn_{0.95}Cr_{0.25}(VFe)_{0.3}$ alloys at different temperatures, and the measurement results are summarized in **table 3**. For as-cast samples, the H_f and S_f don't change very much when the temperature increases from 273 K to 313 K, but the P_a and P_d

promptly increase. However, after annealing, the P_a and P_d increase only slightly with increasing temperature. As a result, C_a, C_d and C_e don't decrease but increase from 1.40%, 1.12% and 0.57% to 2.03%, 1.85% and 1.12% respectively at 313 K. Moreover, comparing to as-cast samples, the annealing samples have a lower plateau pressure. Especially, at 313 K, the P_a decreases from 1.37 MPa to 0.36 MPa, and the P_d decreases from 1.01 MPa to 0.27 MPa. These results can be attributed to annealing treatment, which improve the phase homogeneity and increase the lattice constant. An increase of lattice constants causes the increase of interstitial site, which logically decreases the plateau pressure. However, annealing can't decrease the hysteresis and sloping factor, which is contrary to that reported in the reference [6].

Table 2 PCT measurement results of as-cast $TiMn_{1.25-x}Cr_{0.25}(VFe)_x$ alloys at 273 K

Sample	Hydrogen capacity / %			Plateau pressure /MPa (at H/M=0.5)		Hysteresis factor H_f (at H/M=0.5)	Sloping factor S_f	
	C_a	C_d	C_e	P_a	P_d		S_a	S_d
x=0	1.33	1.06	0.71	2.352	0.508	0.66	0.92	0.79
x=0.1	1.89	1.57	0.83	0.415	0.247	0.23	1.29	1.19
x=0.2	1.95	1.61	0.85	0.351	0.190	0.27	1.20	1.25
x=0.3	2.00	1.69	0.89	0.158	0.114	0.14	1.41	1.65
x=0.4	1.95	1.37	0.77	0.125	0.080	0.19	2.06	1.45

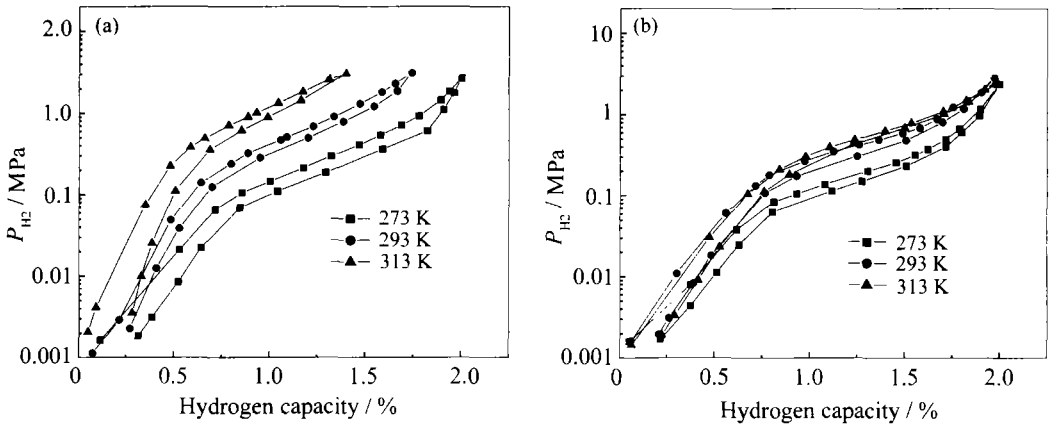

Figure 5 PCT curves of $TiMn_{0.95}Cr_{0.25}(VFe)_{0.3}$ alloys at different temperatures: (a) as-cast; (b) annealed.

Table 3 PCT measurement results of $TiMn_{0.95}Cr_{0.25}(VFe)_{0.3}$ alloys at different temperatures

Temperature / K	Hydrogen capacity / %			Plateau pressure / MPa (at H/M=0.5)		Hysteresis factor H_f (at H/M=0.5)	Sloping factor S_f	
	C_a	C_d	C_e	P_a	P_d		S_a	S_d
273 (as-cast)	2.00	1.69	0.89	0.158	0.114	0.14	1.41	1.65
273 (annealing)	2.00	1.83	0.89	0.131	0.094	0.14	1.40	1.66
293 (as-cast)	1.74	1.43	0.82	0.467	0.351	0.12	1.43	1.50
293 (annealing)	1.97	1.81	1.01	0.304	0.214	0.15	1.45	1.53
313 (as-cast)	1.40	1.12	0.57	1.369	1.011	0.13	1.06	1.43
313 (annealing)	2.03	1.85	1.12	0.360	0.272	0.13	1.05	1.42

4 Conclusions

(1) With increasing VFe substitution for Mn, the lattice constant of the $TiMn_{1.25-x}Cr_{0.25}(VFe)_x$ alloys increase.

(2) For $Ti(MnCrVFe)_{1.5}$ alloys, VFe substitution for Mn increases the hydrogen storage capacity, decreases the plateau pressure and hysteresis. It also results in an increase of slope of the pressure plateau.

(3) Annealing treatment at 1223 K for 6 h can further improve the hydrogen storage characteristics at 273, 293 and 313 K, which attributed to the improvement of phase homogeneity and the increase of lattice constant.

(4) Annealed $TiMn_{0.95}Cr_{0.25}(VFe)_{0.3}$ alloy has a higher hydrogen storage capacity, a lower hydrogen absorptoin-desorption plateau pressure and a smaller hysteresis at 313 K, which is suitable for hydrogen

storage tanks for PEMFC.

References

[1] Y. Morita, T. Gamo, and S. Kuranaka, Effects of nonmetal addition on hydriding properties for Ti-Mn Laves phase alloys [J], *J. Alloys Compd*, 253-254(1997), p.29.

[2] K. Morii and T. Shimizu, Hydriding characteristics in (Ti Zr)(Ni, Mn X)$_2$ alloys [J], *J. Alloys Compd.*, 1-2(1995), p.524.

[3] J.Y. Lee, B.H. Liu, and D.M. Kim, *et al.*, Hydrogen storage properties of $TiMn_2$-based alloys [J], *J. Alloys Compd.*, 240(1996), p.214.

[4] J.G. Park, H.Y. Jang, and S.C. Han, *et al.*, Hydrogen storage properties of $TiMn_2$-based alloys for metal hydride heat pump [J], *J. Mater. Sci. Eng. A*, 329-331(2002), p.351.

[5] Y. Nakamura, H. Nakamura, and S. Fujitani, *et al.*, Characteristics of a hydrogen-absorbing alloy developed for a portable fuel cell [J], *J. Alloys Compd.*, 231(1995), p.898.

[6] Y. Moriwaki, T. Gamo, and T. Lwaki, Control of hydrogen equilibrium pressure for C14-type Laves phase alloys [J], *J. Less-Common Met*, 172-174(1991), p.1028.

[7] C.M. Hong, D.G. Hao, and Q.Z. Lin, Characteristics of hydrogen absorption and reactivation of $TiMn_{1.25}Cr_{0.25}$ alloy [J], *J. Less-Common Met*, 172-174(1991), p.1044.

[8] Y.H. Xu, C.P. Chen, and X.L. Wang, *et al.*, The cycle life and surface properties of Ti-based AB_2 metal hydride electrodes [J], *J. Alloys Compd.*, 337(1996), p.216.

[9] J.L. Bobet and B. Darriet, Relationship between hydrogen sorption properties and crystallography for $TiMn_2$ based alloys [J], *Int. J. Hydrogen Energy*, 25(2000), p.769.

[10] H.H. Lee, K.Y.Lee, and J.Y. Lee, The Ti-based metal hydride electrode for Ni-MH rechargeable batteries [J], *J. Alloys Compd.*, 239(1996), p.63.

[11] C.B. Jung and K.S. Lee, The effect of heat treatment on the electrode characteristics of the ball-milled Zr-Cr-Ni [J], *J. Alloys Compd.*, 274(1998), p.254.